Spin-spin dependence of the total cross section of ^{59}Co for neutrons up to 31 MeV

W. Heeringa and H. Postma
*Laboratorium voor Algemene Natuurkunde, Rijksuniversiteit Groningen, The Netherlands**

H. Dobiasch,† R. Fischer,† H. O. Klages,† R. Maschuw, and B. Zeitnitz†
II. Institut für Experimentalphysik, Universität Hamburg, Germany‡

(Received 22 February 1977)

The spin-spin dependence of the total cross section of ^{59}Co for neutrons was measured at seven energies. A polarized neutron beam with energies of 8.2, 11.1, 12.8, and 14.1 MeV from the ^{2}H$(d,\vec{n})^3$He reaction and of 23.0, 27.5, and 30.6 MeV from the ^{3}H$(d,\vec{n})^4$He reaction was transmitted through a cobalt sample. The cobalt target was cooled with a ^{3}He-^{4}He dilution refrigerator and polarized in a magnetic field. The transmission rates of the neutrons were compared for parallel and antiparallel spin orientations. The values obtained for the spin-spin cross section are much smaller than those found below 3 MeV. Deduced strengths of spin-spin terms in the optical model are in the range of 1 MeV. This is of the same order of magnitude as estimated from microscopic calculations.

[NUCLEAR REACTIONS $^{59}\vec{\text{Co}}+\vec{n}$, E_n = 8–31 MeV; measured spin-spin dependent transmission; deduced σ_{ss}; deduced optical model spin-spin terms.]

I. INTRODUCTION

Since Feshbach[1] suggested the inclusion of a spin-spin term in the optical potential, several experimental and theoretical attempts have been made to determine the properties of this term. Two different experimental methods were applied:

(i) measurement of the depolarization of polarized nucleons scattered by unpolarized nuclei,[2-6]
(ii) transmission measurements determining the difference in total cross section of polarized nuclei for polarized neutrons with parallel and antiparallel spin orientations.[7-13]

The extraction of a spin-spin term from depolarization measurements is complicated by other mechanisms. For nuclei with spin $I>\frac{1}{2}$, quadrupole spin-flip can occur and for low bombarding energies contributions from compound-elastic scattering to the depolarization may be important. Recent calculations[14,15] show that the existing experimental results can be described without a spin-spin term. Hence a transmission measurement seems to be a more precise method, at present, to determine the nucleon-nucleus spin-spin term. In this experiment the measured quantities are the counting rates of the transmitted neutrons with spins parallel (N_p) and antiparallel (N_a) to the spins of the target nuclei. The transmission effect ϵ is defined as $\epsilon=(N_p-N_a)/(N_p+N_a)$. For small values of ϵ the spin-spin dependent part of the total cross section can be written as

$$\sigma_{ss}=-\epsilon/(P_n P_t NL). \quad (1)$$

Here P_n and P_t are the neutron and target polarizations, respectively, N is the target density and L the target length.

In a previous letter[13] we reported on measurements using polarized ^{59}Co nuclei and polarized neutrons in the energy range 0.4–2.9 MeV. Optical model calculations fail to fit these data in the entire energy range. Separate fits to parts of the data give results for the spin-spin term that differ in sign. Moreover, the absolute values are about an order of magnitude larger than theoretical estimates.[11,16] It was shown by Thompson[17] that the data at these low energies might be explained by compound-nucleus effects only. In this paper we report on a continuation of these measurements to higher energies where compound-nucleus effects are assumed to be unimportant. The measurements were performed at seven energies between 8.2 and 30.6 MeV.

II. EXPERIMENTAL ARRANGEMENT AND PROCEDURE

A schematic view of the experimental arrangement is shown in Fig. 1. The deuteron beam of the 30-MeV cyclotron of the University of Hamburg was used to produce neutrons utilizing the reactions ^{2}H$(d,\vec{n})^3$He and ^{3}H$(d,\vec{n})^4$He. The neutrons emerging at an angle of 30° with respect to the incoming deuterons were collimated by heavy shielding. The neutron beam passed the field of a superconducting solenoid which rotated the direction of the neutron spins. The ^{59}Co target was a 210-g single crystal, which was cooled to 0.05 K and magnetized in the field of a superconducting split

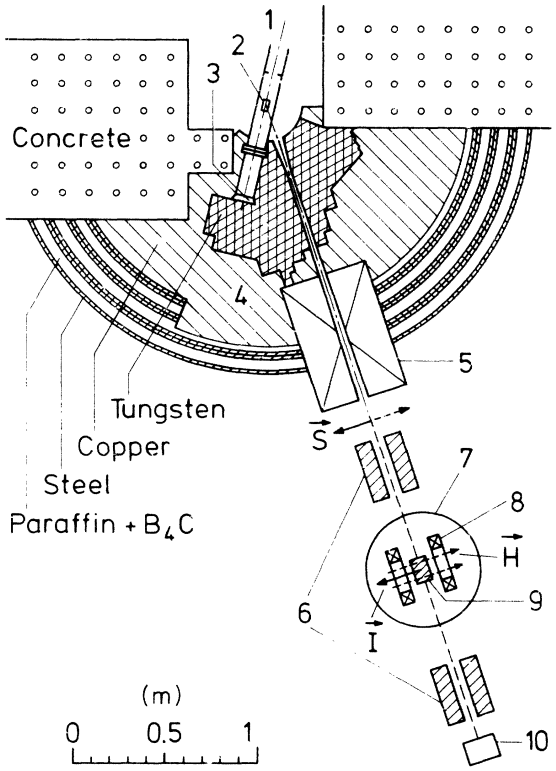

FIG. 1. View of the experimental setup. The drawing denotes a cross section through the horizontal plane: 1—deuteron beam, 2—gas target cell, 3—Faraday cup, 4—shielding, 5—superconducting solenoid, 6—heavy metal collimators, 7—cryostat mantle, 8—superconducting magnet, 9—cobalt target, and 10—neutron detector; $\vec{s}$—neutron spin, which lies in the horizontal plane after passage through the solenoid, $\vec{H}$—field of the superconducting magnet, and $\vec{I}$—spin of the cobalt nuclei. $\vec{I}$ is antiparallel to $\vec{H}$ because of the negative value of the internal field at the cobalt nuclei.

coil magnet. The resulting spin orientations for the neutron beam and the target are also shown in Fig. 1. The transmitted neutrons were detected with a liquid scintillator using pulse-shape discrimination techniques. The energy of the neutrons was measured by the time-of-flight method. A second time-of-flight spectrometer was used at a different neutron production angle to monitor the flux from the neutron source.

A. Polarized neutron beam

The target and collimator arrangement for the production of a monoenergetic polarized neutron beam has been described in detail elsewhere.[18] The gas target cell was a steel cylinder with molybdenum windows, filled with $^2H_2$ and $^3H_2$, respectively, and cooled by liquid nitrogen. The target area was surrounded by shielding composed of concrete, tungsten, copper, iron, and paraffin.[19] A transmission channel at 30° with respect to the incoming deuterons gave a collimated neutron beam of about 5-cm diam. The superconducting solenoid for the rotation of the neutron spins was part of the shielding. The neutron beam was collimated once more to a diameter of approximately 15 mm to make sure that it was shadowed from the detector by the cobalt target. The distance between the neutron source and the cobalt target was 280 cm.

TABLE I. Results of the spin-spin cross section of polarized ^{59}Co for polarized neutrons ($P_t = 0.28 \pm 0.03$, $NL = 3.4 \times 10^{23}$ nuclei/cm^2).

E_n (MeV)	P_n (%)	ϵ (parts per thousand)	σ_{ss} (mb)
8.2 ± 0.1	11.0 ± 1.5	−0.9 ± 1.1	+86 ± 112
11.1 ± 0.1	35.0 ± 0.8	−0.4 ± 0.9	+12 ± 28
12.8 ± 0.1	43.0 ± 0.7	1.7 ± 0.9	−42 ± 23
14.1 ± 0.1	43.5 ± 0.7	0.3 ± 0.8	−7 ± 19
23.0 ± 0.1	60 ± 2	−0.4 ± 0.9	+7 ± 16
27.5 ± 0.1	72 ± 3	−0.1 ± 1.9	+1 ± 28
30.6 ± 0.1	68 ± 4	−3.2 ± 1.6	+49 ± 25

The polarization of our neutron beam produced by the reaction $^2H(d,\vec{n})^3He$ was measured with a liquid-^{4}He polarimeter at five deuteron energies from 8 to 16 MeV.[20] Calculations at neutron energies of 15 and 30 MeV[21] showed that in our experimental arrangement the depolarization effects caused by Mott-Schwinger scattering are very small. For the neutron energies above 16 MeV we may therefore use the neutron polarization data from the literature.[22] The values of the beam polarization applied in our analysis are listed in Table I.

B. Polarized cobalt target

The cobalt target was a 210 g, approximately cylindrical, single crystal of 5% Fe and 95% Co with a length of 40 mm and a diameter varying from 26 to 29 mm. The neutron beam direction was parallel to the longitudinal axis of the sample. For this arrangement the effective target thickness is $NL = 3.4 \times 10^{23}$ nuclei/cm^2.

The target was cooled to about 50 mK in a ^{3}He-^{4}He dilution refrigerator built at the physics laboratory in Groningen. A schematic drawing of the lower part of the refrigerator is shown in Fig. 2. Its construction was roughly the same as that of the one described in Ref. 23. More details of the cryostat and the target assembly will be given in Ref. 27. A split-coil superconducting magnet was connected to the bottom of the 4-K bath. The cobalt sample was magnetized in a direction of easy magnetization perpendicular to the longitudinal axis by applying a field of about 0.9 T. The polarization was determined by measuring the anisotropy of the γ radiation of a small amount of ^{60}Co (5 μCi) which

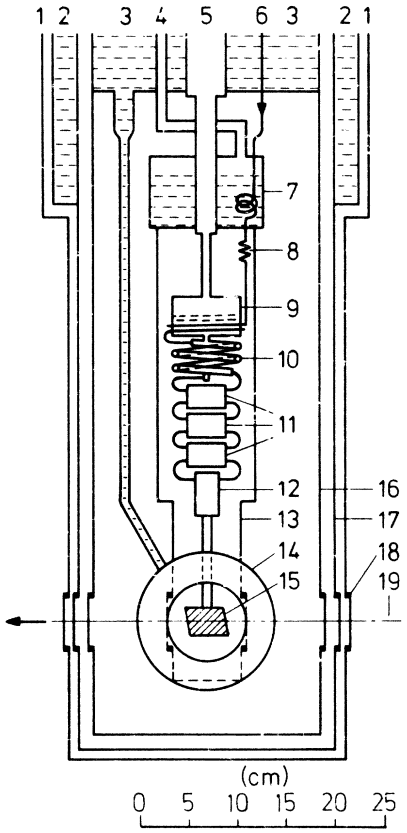

FIG. 2. Schematic drawing of the lower part of the dilution refrigerator: 1—outer mantle, 2—liquid nitrogen reservoir, 3—4.2-K liquid helium bath, 4—pumping tube for 1.0-K liquid helium bath, 5—^{3}He pumping tube, 6—^{3}He return line, 7—1.0-K helium bath, 8—flow impedance, 9—^{3}He evaporator, 10—continuous heat exchanger, 11—step heat exchangers, 12—mixing chamber, 13—1-K shield, 14—superconducting magnet, 15—cobalt target, 16—4-K shield, 17—77-K shield, 18—windows, and 19—neutron beam direction.

has been produced in the target by activation in a reactor. The deduced target polarization during this experiment is $P_t = 0.28 \pm 0.03$. During the neutron transmission experiments the temperature was monitored by carbon resistors.

C. Neutron detection and acquisition of data

The neutrons transmitted through the cobalt sample passed a third carefully positioned collimator of heavy metal, which shielded the detector against the neutrons scattered in the sample. The detector was a 10-cm diam × 7.5-cm long liquid scintillator (NE 213), which was viewed by a fast photomultiplier (Valvo XP 2041). The neutron energy was measured by the time-of-flight method. A signal derived from the cyclotron radio-frequency served as a time reference. The overall time resolution full width at half maximum was 1.5 to 2.0 nsec.

The discrimination against γ rays was done using the zero-crossing method. We set a rough electronic threshold in this pulse-shape spectrum to avoid high counting rates from γ rays in the analog-to-digital converters.

For each accepted event three pieces of information were stored on magnetic tape using a PDP-9 computer: (a) the time-of-flight (TOF) between neutron source and detector, (b) the analog pulse-shape (PS) information, and (c) the energy (E) of the recoiled particle in the detector. The projections of the three-dimensional data could be observed during the experiment. This allowed the detection of changes in the spectra due to variations of the cyclotron beam, the gas target, or the detection system. Figure 4 shows the important parts of these projections for a run of about 1000 sec at a neutron energy of 8.2 MeV. The arrows indicate typical lower and upper limits used in the data re-

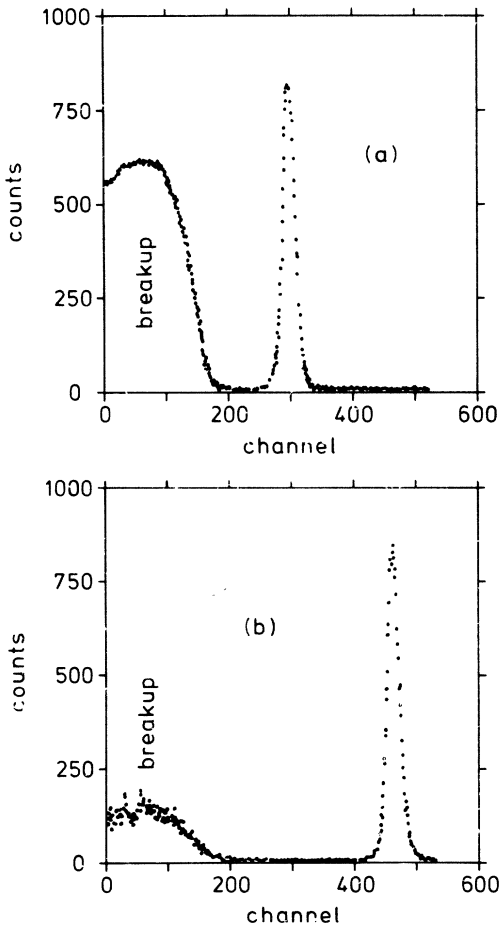

FIG. 3. Time-of-flight spectra of the neutrons produced by the ^{2}H(d,n) reaction [(a) $E(n_0) = 14.1$ MeV] and the ^{3}H(d,n) reaction [(b) $E(n_0) = 30.6$ MeV], respectively. The flight path from the gas target to the detector was 320 cm.

duction. The monitor was a similar TOF spectrometer with pulse-shape discrimination and a fixed lower energy level. These TOF spectra were also stored in the PDP-9 computer during each transmission measurement.

To suppress the influence of time dependent changes in the apparatus the field of the superconducting solenoid was reversed each time a charge of 10^{-3} C was collected. This gave runs of about 1000 sec at the typical beam current of approximately 1 μA. Depending on the neutron energy, 10^4 to 10^5 accepted transmission events were collected in this time interval. The monitor counting rate was about a factor of 100 higher.

Control measurements were performed with the target unpolarized to look for instrumental asymmetries. For example, a misalignment of the third heavy metal collimator would cause an apparent asymmetry due to the high analyzing power of Mott-Schwinger scattering for small angles. For this purpose the cobalt sample was brought to a temperature of 1.0 K. The polarization of the sample at 1.0 K is completely negligible in our case. Nothing else was changed compared to the "cold" measurements. The counting rates for the "warm" and the "cold" measurements were of the same order of magnitude.

As can be seen already from the original TOF projections (Fig. 3) the peak-to-background ratio was very high due to the clean spectra from the neutron source. Background measurements were performed with a piece of heavy metal inserted in the path of the neutron beam as a total attenuator. The very small background was flat in the region of the TOF peak.

III. EXPERIMENTAL RESULTS

The first step in the data reduction was to find the minimum between the neutron and γ peak in the PS spectrum [Fig. 4(b)] by fitting the region around the minimum with a parabola. Then lower and upper levels were set in the E spectrum [Fig. 4(c)]. The upper level limited the high-energy tail where pile-up events and amplifier saturation may occur. Three different lower levels were used for a consistency check. Firstly, the hardware level, secondly, a slightly higher level which removes the usually quite steep slope at the beginning of the spectrum (5–10% of the counts), and, thirdly, a much higher level which removes 20–50% of the counts. Then all events between the levels in the PS and E spectra were projected on the TOF axis. The TOF spectra for both relative spin orientations were summed separately and a linear background subtraction was performed.

In this way three values of ϵ were obtained at each neutron energy corresponding to the three lower energy levels. These numbers were found to be consistent within statistics. Usually, the integrated deuteron current was adequate for normalization. In only two of the 420 runs was it necessary to rely on the monitor counter, because the pressure in the gas target had considerably changed during the runs due to ineffective cooling. The final results of the experiment are shown in Table I. The errors in ϵ are statistical. In σ_{ss} the uncertainties of the beam and target polarization, respectively, are taken into account. No corrections have been made for finite geometry effects since the distances between neutron source, tar-

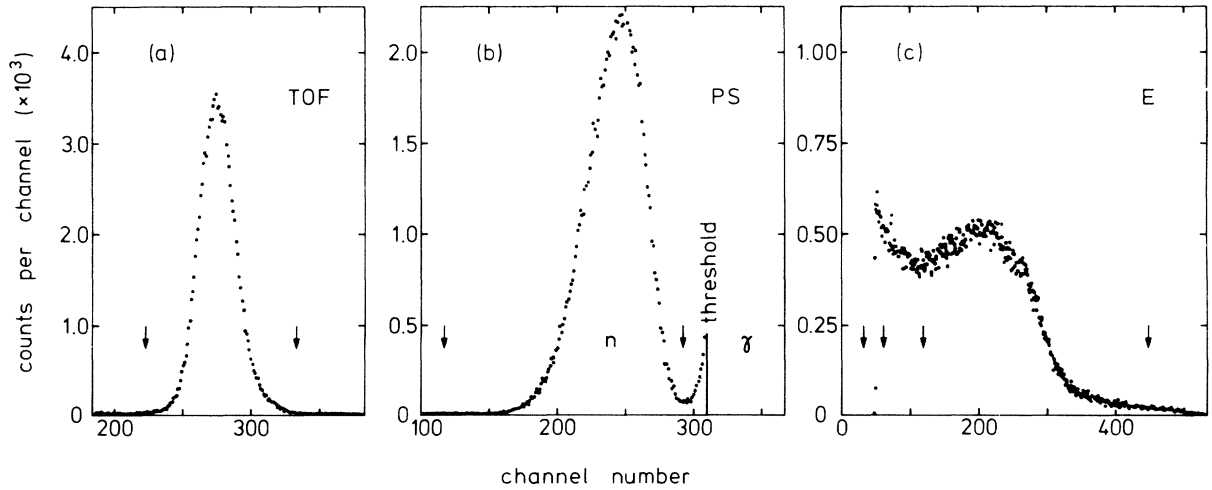

FIG. 4. Projections of a 3-dimensional neutron spectrum at 8.2 MeV: (a) part of the time-of-flight axis with the ^{2}H(d,n)^{3}He-neutron peak, (b) n-γ discrimination spectrum with electronic threshold in the γ region, and (c) proton recoil energy distribution. The arrows indicate lower and upper limits used in the data reduction.

TABLE II. Results of control measurements with unpolarized target ($NL = 3.4 \times 10^{23}$ nuclei/cm^2).

E_n (MeV)	P_n (%)	ϵ (parts per thousand)	ϵ/P_nNL (mb)
8.2±0.1	11.0±1.5	−1.5±0.9	−41 ±24
11.1±0.1	35.0±0.8	−0.3±1.0	−2.5±8.4
12.7±0.1	43.0±0.7	−0.6±1.1	−4.2±7.6
14.2±0.1	43.5±0.7	0.9±0.9	6.2±6.2
23.0±0.1	60 ±2	−1.5±1.0	−7.3±5.0

get, and detector were large. A statistical combination of the measurements with unpolarized target listed in Table II yields $\epsilon/(P_nNL) = -3.1 \pm 3.6$ mb. Therefore we assume that false asymmetries were not important in this experiment.

IV. OPTICAL MODEL CALCULATIONS

In Fig. 5 the results of σ_{ss} from Table I are shown together with energy averaged values obtained from previous measurements at lower energies.[13] It has been found[12] that the low-energy data (<3 MeV) cannot be reproduced using a spin-spin term in the optical potential. A recent estimate[17] shows that at these low energies (where the compound-nucleus levels are isolated) the measured effects may be explained by a compound-nucleus absorption model. The levels of the compound nucleus start to overlap strongly with increasing energy. Using results from Refs. 28 and 29 for the level width Γ and from Ref. 30 for the level density D, it is found that Γ/D increases from $\Gamma/D \simeq 0.3$ at $E_n = 1$ MeV to $\Gamma/D \simeq 300$ at $E_n = 10$ MeV for levels of definite spin and parity ($J^\pi = 3^-$ or 4^-). The compound-nucleus absorption model that reproduces the spin-spin effects at low energies does not apply in the region of strongly overlapping levels and we assume that the effects are averaged out in that region. Moreover, compound-nucleus formation decreases above 10 MeV because of the increasing importance of direct nonelastic processes.[31] Therefore, we assume that compound-nucleus spin-spin effects are negligible in the energy range of our measurements. In that case the data may be compared with calculations using optical model spin-spin terms.

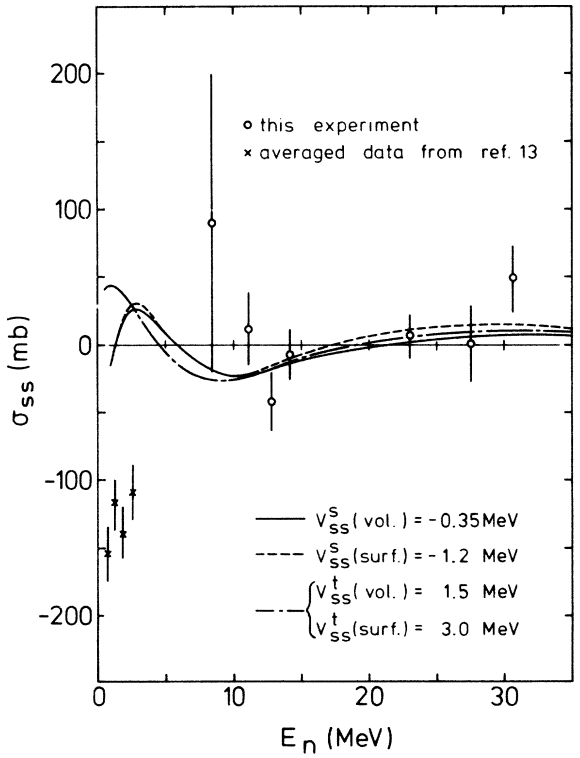

FIG. 5. Fits to the spin-spin cross section of ^{59}Co for neutrons using different spin-spin terms in the optical potential. Low energy data from Ref. 13 are averaged over energy intervals of 500 keV.

The two simplest invariant forms of a spin-spin term are the spherical form (2a) and the tensor form (2b):

$$U^s_{ss}(r) = -V^s_{ss} F_s(r) \vec{\sigma} \cdot \vec{I}/I , \tag{2a}$$

$$U^t_{ss}(\vec{r}) = -V^t_{ss} F_t(\vec{r}) [3(\vec{\sigma} \cdot \hat{r})(\vec{I} \cdot \hat{r}) - \vec{\sigma} \cdot \vec{I}]/2I . \tag{2b}$$

The strengths V^s_{ss} and V^t_{ss} are expected to be small compared to the other terms in the optical potential so σ_{ss} can be calculated using distorted wave Born approximation (DWBA). Calculations were carried out with the DWBA code SPINSOR[24] provided by Sherif. This code computes the scattering amplitudes in the presence of a spin-spin interaction and calculates the Wolfenstein parameters as a function of angle.

The spin-spin cross section can be written as[10]:

$$\sigma_{ss} = \frac{4\pi}{kP_nP_t} \operatorname{Im} \operatorname{Tr} [\rho^t \rho^n f_s(0^\circ)] . \tag{3}$$

Here ρ^t and ρ^n are the density matrices for the target and incident neutrons and f_s is the spin-spin dependent part of the scattering amplitude. The code SPINSOR was extended to calculate σ_{ss} according to Eq. (3).

Calculations by Fisher *et al.*[12] revealed that variations of the optical model parameters do not change the results for σ_{ss} essentially at neutron energies above 8 MeV. This was confirmed by our calculations, hence we omit this topic in our discussion. The optical model parameters used were those of Wilmore and Hodgson[25] for neutron energies below 12 MeV and of Becchetti and Greenlees[26] for higher energies. Calculations were performed with the spherical term and the tensor term separately. In both cases two radial form factors

were used, of Woods-Saxon (volume) and of Woods-Saxon derivative (surface-peaked) shape.

For the volume shape we took the parameters of the central potential of the Becchetti-Greenlees set ($R = 4.55$ fm, $a = 0.75$ fm). Fitting the data to the spherical spin-spin term with these parameters yields $V^s_{ss}(\text{vol.}) = -0.35 \pm 0.25$ MeV and fitting to the tensor term: $V^t_{ss}(\text{vol.}) = 1.5 \pm 1.1$ MeV. The corresponding curves of σ_{ss} as a function of energy are shown in Fig. 5. It can be seen that an acceptable fit to our data and the earlier results below 3 MeV is not possible.

Microscopic calculations concerning the spin-spin potential of ^{59}Co for neutrons were performed by Satchler.[16] In this work the ^{59}Co nucleus was treated as a single proton hole in the $1f_{7/2}$ shell plus a core which can be polarized. The resulting spherical spin-spin term has a surface-peaked shape with a maximum value of −350 keV. [In Ref. 16 the maximum is −100 keV, because there $V_{ss}(r)$ is defined without the factor I in the denominator.] The form of this surface-peaked shape can be well approximated by a Woods-Saxon derivative form with $R = 3.50$ fm and $a = 0.55$ fm. Fits to our data with this shape for the spherical term give $V^s_{ss}(\text{surf.}) = -1.2 \pm 0.8$ MeV. The corresponding curve for σ_{ss} is also shown in Fig. 5. No detailed structure was deduced in Ref. 16 for the tensor term. It was concluded that its strength is probably less than 0.1 MeV. A fit with the tensor term with surface-peaked shape gives $V^t_{ss}(\text{surf.}) = 3.0 \pm 2.0$ MeV. The curve obtained coincides with the curve for $V^t_{ss}(\text{vol.}) = 1.5$ MeV.

V. CONCLUSIONS

In the past decade several experiments were performed in order to determine a spin-spin term in the optical model. Recently it became clear, however, that the results of almost all these measurements are questionable due to the presence of other mechanisms that may have caused the measured effects. The explanation of the existing depolarization data is complicated by the occurrence of quadrupole spin-flip and by depolarization through compound-elastic scattering.

All earlier transmission experiments were performed with neutrons below 3 MeV (except two single data points at 8 MeV). At these low energies spin-spin effects can appear due to differences in the compound-nucleus absorption cross section for parallel and antiparallel spin orientations. The transmission data presented here were obtained at seven neutron energies between 8 and 31 MeV. We found much smaller values for the spin-spin cross section than those obtained below 3 MeV. Presumably the compound-nucleus spin-spin effects have disappeared above 8 MeV. In comparing our data with optical model calculations, different kinds of spin-spin terms were used. The deduced strengths were of the order of 1 MeV.

From our measurements alone it is not possible to conclude whether the spherical or the tensor spin-spin term is dominating. It has been shown[32] that in order to discriminate between these terms a second transmission experiment has to be performed, this time in the longitudinal geometry. This means that the spins should be parallel or antiparallel to the neutron direction of flight (our experiment was performed in perpendicular geometry). It seems reasonable, however, to assume that the contribution of the tensor term is less important. Firstly, the estimates in Ref. 16 indicate that the tensor strength is smaller than the spherical strength. Secondly, it appears from the calculations that a tensor term with the same strength as the spherical term produces smaller spin-spin effects. If we consider only the spherical term, the experimental value of the strength $V^s_{ss}(\text{surf.}) = -1.2 \pm 0.8$ MeV can be compared with the theoretical value +0.35 MeV from Ref. 16.

ACKNOWLEDGMENTS

The authors wish to thank A. H. J. Timans for his help with the construction of the cryostat and with setting up the cryostat at the Hamburg cyclotron. We gratefully acknowledge the assistance of B. Haesner during the data taking, of F. Kienle for preparing the tritium target, and of H. Riege for assistance with the data handling.

*Work supported by the Nederlandse Organisatie voor Zuiver Wetenschappelijk Onderzoek (ZWO) through the Stichting voor Fundamenteel Onderzoek der Materie (FOM).

†Now at University of Bochum, Germany.

‡Work supported by the Bundesministerium für Forschung und Technologie.

[1]H. Feshbach, Annu. Rev. Nucl. Sci. 8, 49 (1958).

[2]K. Katori, T. Nagata, A. Uchida, and S. Kobayashi, J. Phys. Soc. Jpn. 28, 1116 (1970).

[3]C. J. Batty and C. Tschalär, Nucl. Phys. A143, 151 (1970).

[4]R. Beurtey, P. Catillon, and P. Schnabel, J. Phys. (Paris) Suppl. 31, Nos. 5,6, C2-96 (1970); P. Catillon, in *Polarization Phenomena in Nuclear Reactions, Madison, 1970,* edited by H. H. Barschall and W. Haeberli (Univ. of Wisconsin Press, Madison, 1971), p. 657.

[5]J. Birchall, H. E. Conzett, J. Arvieux, W. Dahme, and R. M. Larimer, Phys. Lett. 53B, 165 (1974).

[6]M. P. Baker, J. S. Blair, J. G. Cramer, T. Trainor,

and W. Weitkamp, in *Proceedings of the Fourth International Symposium on Polarization Phenomena in Nuclear Reactions, Zürich, 1975*, edited by W. Grüebler and V. König (Birkhäuser, Basel, 1976), p. 628; J. Birchall, H. E. Conzett, F. N. Rad, S. Chintalpudi, and R. M. Larimer, *ibid.*, p. 630; T. B. Clegg, W. J. Thompson, R. A. Hardekopf, and G. G. Ohlsen, *ibid.*, p. 634.

[7]R. Wagner, P. D. Miller, T. Tamura, and H. Marshak, Phys. Rev. 139, B29 (1965).

[8]T. R. Fisher, R. S. Safrata, E. G. Shelley, J. McCarthy, S. M. Austin, and R. C. Barrett, Phys. Rev. 157, 1149 (1967).

[9]S. Kobayashi, H. Kamitsubo, K. Katori, A. Uchida, M. Imaizumi, and K. Nagamine, J. Phys. Soc. Jpn. 22, 368 (1967).

[10]T. R. Fisher, D. C. Healey, and J. S. McCarthy, Nucl. Phys. A130, 609 (1969).

[11]K. Nagamine, A. Uchida, and S. Kobayashi, Nucl. Phys. A145, 203 (1970).

[12]T. R. Fisher, H. A. Grench, D. C. Healey, J. S. McCarthy, D. Parks, and R. Whitney, Nucl. Phys. A179, 241 (1972).

[13]W. Heeringa and H. Postma, Phys. Lett. 61B, 350 (1976).

[14]J. S. Blair, M. P. Baker, and H. S. Sherif, Phys. Lett. 60B, 25 (1975).

[15]W. J. Thompson, Phys. Lett. 62B, 245 (1976).

[16]G. R. Satchler, Particles and Nuclei 1, 397 (1972); Phys. Lett. 34B, 37 (1971).

[17]W. J. Thompson, Phys. Lett. 65B, 309 (1976).

[18]R. Fischer, F. Kienle, H. O. Klages, R. Maschuw, and B. Zeitnitz, Nucl. Phys. A282, 189 (1977); and in *Proceedings of the Fourth International Symposium on Polarization Phenomena in Nuclear Reactions, Zürich, 1975* (see Ref. 6), p. 835.

[19]R. Fischer, University of Hamburg, 1973 (unpublished).

[20]R. Schrader, Ph.D. thesis, University of Hamburg, 1975 (unpublished); R. Fischer, F. Kienle, H. O. Klages, R. Maschuw, R. Schrader, P. Suhr, and B. Zeitnitz, in *Proceedings of the Fourth International Symposium on Polarization Phenomena in Nuclear Reactions, Zürich, 1975* (see Ref. 6), p. 835.

[21]R. Fischer, R. Maschuw, R. Schrader, and B. Zeitnitz, Nucl. Instrum. Methods 136, 105 (1976).

[22]G. S. Mutchler, W. B. Broste, and J. E. Simmons, Phys. Rev. C 3, 1031 (1971).

[23]H. Postma, Nucl. Instrum. Methods 88, 45 (1970).

[24]A. H. Hussein and H. S. Sherif, Phys. Rev. C 8, 518 (1973).

[25]D. Wilmore and P. E. Hodgson, Nucl. Phys. 55, 673 (1964).

[26]F. D. Becchetti, Jr., and G. W. Greenlees, Phys. Rev. 182, 1190 (1969).

[27]W. Heeringa, Ph.D. thesis, University of Groningen (unpublished).

[28]T. Ericson and T. Mayer-Kuckuk, Annu. Rev. Nucl. Sci. 16, 183 (1966).

[29]*Resonance Parameters*, compiled by S. F. Mughabghab and D. I. Garber, Brookhaven National Laboratory Report No. BNL-325 (National Technical Information Service, Springfield, Virginia, 1973), 3rd ed., Vol. 1.

[30]A. Gilbert and A. G. W. Cameron, Can. J. Phys. 43, 1446 (1965).

[31]A. A. Luk'yanov, O. A. Sal'nikov, and E. M. Saprykin, Yad. Fiz. 21, 67 (1975) [Sov. J. Nucl. Phys. 21, 35 (1975)].

[32]T. R. Fisher, Phys. Lett. 35B, 573 (1971).